

Study on local structure around Ce and Gd atoms in CeO₂-Gd₂O₃ binary system

Takashi Nakagawa,^a Takahiro Osuki,^a Takao A. Yamamoto,^a Yoshiyasu Kitauji,^a Masataka Kano,^a Masahiro Katsura,^a and Shuichi Emura^b

^aDepartment of Nuclear Engineering, Graduate School of Engineering, Osaka University, 2-1 Yamadaoka, Suita, Osaka 565-0871, Japan, ^bThe Institute of Scientific and Industrial Research, Osaka University, Mihogaoka 8-1, Ibaraki, Osaka 567-0047, Japan

X-ray absorption spectra near Ce and Gd *K*-edges of binary oxide of Ce_xGd_{1-x}O_{(3+x)/2} (0 ≤ *x* ≤ 0.5) in C-type structure solid solution were measured by use of the beamline BL01B1 at SPring-8. Interatomic distances between rare-earth and oxygen atoms, *R*_{Gd-O} and *R*_{Ce-O}, were evaluated with the extended x-ray absorption fine structure analysis and found to increase with *x*. *R*_{Gd-O} was larger than *R*_{Ce-O} by about 0.1 Å. Metal-oxygen distances estimated as their linear combinations, *xR*_{Ce-O} + (1-*x*)*R*_{Gd-O}, well agreed with those determined by X-ray diffraction.

Keywords: CeO₂, Gd₂O₃, C-type structure, K-edge, XAFS

1. Introduction

Cerium dioxide, CeO₂, has fluorite structure (CaF₂ type) in which eight oxygen atoms surround a cerium atom. Gadolinium sesqui-oxide, Gd₂O₃, has C-type crystal structure (Mn₂O₃ type) in which six oxygen atoms surround a gadolinium atom. C-type structure is obtained by removing two oxygen atoms of eight in fluorite structure in a regular manner. In CeO₂-Gd₂O₃ binary systems, single phase of fluorite structure oxide appears in Ce-rich region. C-type monophasic is obtained in Gd-rich region. The diphasic region separates the fluorite solid solution from the C-type phase. Gadolinia-doped ceria has been known as a good ionic conductor due to oxygen vacancies introduced by the doping (Kudo & Obayashi, 1975, Inaba & Tagawa, 1996). The local structures around metal atoms in this binary oxide have been extensively investigated in order to study correlation with the ionic conduction behavior. Ohashi *et al.* (1998) reported Ce- and Gd-O interatomic distances and location of vacancy in fluorite-type oxide of Ce_xGd_{1-x}O_{(3+x)/2} (*x* ≥ 0.7) by examining Ce and Gd *L*_{III}-edge X-ray absorption fine structure (XAFS). Inaba *et al.* (1999) calculated the interatomic distances and coordination numbers of oxygen around rare-earth atoms in Ce_xGd_{1-x}O_{(3+x)/2} (*x* ≥ 0.85) by means of molecular dynamics simulation. However, little attention has been paid on the local structures in a region of smaller *x*.

The rare-earth *K*-edge XAFS measurements can provide more reliable data for the EXAFS (Extended X-ray Absorption Fine Structure) analysis, because an energy separation between adjacent elements' *K*-edges is far larger than that between *L*_{III}- and *L*_{II}-edges of the relevant rare-earth element (Nakagawa *et al.*, 1999). The wider energy separation leads to wave-number data

over a wider region, which is favorable to EXAFS analysis. Objective of this work is to examine the local structures around Gd and Ce atoms in CeO₂-Gd₂O₃ solid solutions in a Gd-rich region (0 ≤ *x* ≤ 0.5) with C-type crystal structure. X-ray absorption spectra at both Ce and Gd *K*-edges were measured for these oxides with C-type structure.

2. Experimental

Powders of cerium dioxide (CeO₂, 99.99%) and gadolinium sesqui-oxide (Gd₂O₃, 99.99%) purchased from Rare Metallic Co., Ltd were weighed to adjust a mixing ratio and thoroughly mixed with a set of mortar and pestle made of agate. We have prepared mixtures of CeO₂ and Gd₂O₃ with various mixing ratios *x* (*x* = Ce/(Ce+Gd)). Each powder mixture was pressed under 310 MPa into a disk of 10-mm diameter and 1-mm thickness. The disk was heated in air at 1450°C for 12 hours. The disk was pulverized for preparing a specimen of x-ray powder diffraction (XRD) analysis with Cu-*K*_α radiation. After phase examination with XRD, the powder was again shaped into two disks with proper thicknesses for Ce- and Gd-*K*-edge XAFS measurements. XAFS measurements were carried out in a transmission mode at room temperature at the beamline BL01B1 in SPring-8 (Uruga *et al.*, 1999) using Si (311) plane of double-crystal monochromator and a focusing mirror system. The x-ray beam was of 5 × 1 mm² at the sample position. Step angle of monochromator was 0.0003° and integration time per point was 3 seconds. Energy resolution was 5 eV at Gd *K*-edge (50.2 keV). The x-ray energy of inflection point of the white line at *K*-edge of Gd foil was set 50.235 keV. In the machine-time, no deviation was observed this preset energy although Gd *K*-edge spectra of Gd foil were measured for several times. Oxygen contents in the sample after the heat was analyzed with the inert gas fusion infrared absorption method.

3. Results and discussion

Figure 1 shows the oxygen contents determined by chemical analysis plotted against the mixing ratio *x*. Oxygen contents increase with increasing Ce mixing ratios. The binary oxides are expressed as a chemical formula Ce_xGd_{1-x}O_{(3+x)/2} since the potted

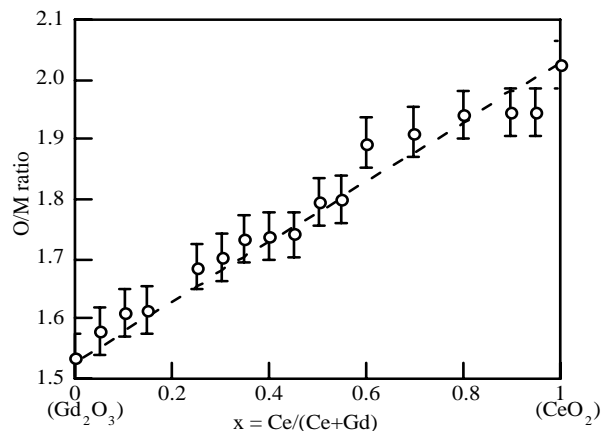


Figure 1

Oxygen contents determined with chemical analysis as a function of rare-earth composition in the reactant powder.

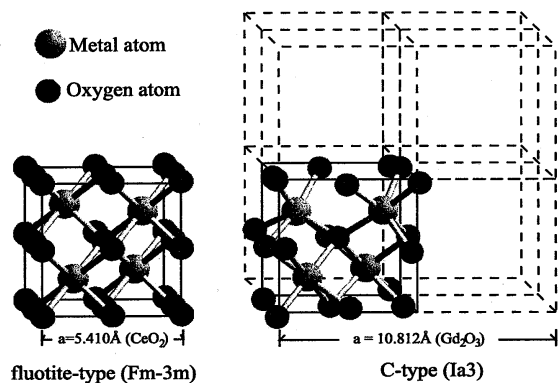


Figure 2
Crystal structures of fluorite- and C-types.

points agree with a straight line drawn between the points of $x = 0$ (Gd_2O_3) and $x = 1$ (CeO_2). X-ray diffraction peaks due to C-type and fluorite-type of $\text{Ce}_x\text{Gd}_{1-x}\text{O}_{(3+x)/2}$ appear at almost same angles because the C-type structure is a superstructure of fluorite with double the cell edge of the latter as shown in Fig. 2. The phases occurring in these binary oxides were determined by examining the peaks of lattice planes, C-type (844) and fluorite type (422). Lattice parameters of these oxides as a function of x are shown in Fig. 3, which indicates that monophasic C-type oxide occurs in a compositional region $x < 0.6$. As x increases, the lattice expands in the monophasic region.

In Fig. 4, Gd K -edge x-ray absorption spectrum obtained at $x = 0.05$ is shown together with x-ray intensities of incident beam I_0 and of the transmitted I , which were monitored by ionization chambers with flowing Kr25%-Ar75% and static Xe gases, respectively. It should be noticed first that a spectrum is observed over an energy range, about 1500 eV, and it is far wider than those obtained by L_{III} -edge measurements which is at most over

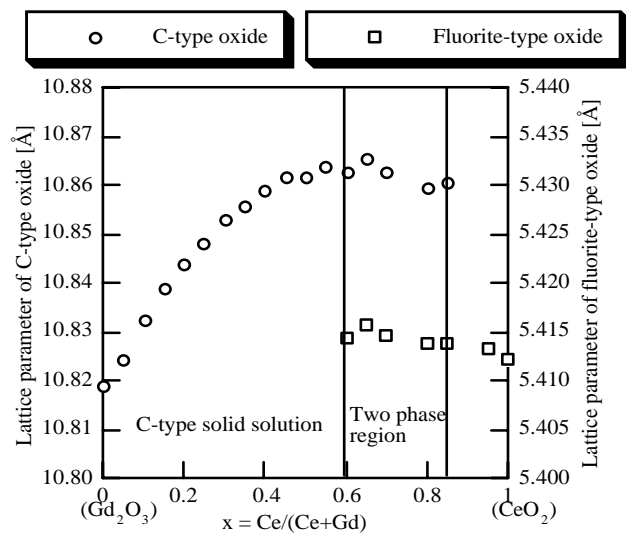


Figure 3
Lattice parameters of C-type and fluorite structures found in CeO_2 - Gd_2O_3 binary oxides. Two phases coexist when $\text{Ce}/(\text{Ce}+\text{Gd}) > 0.6$.

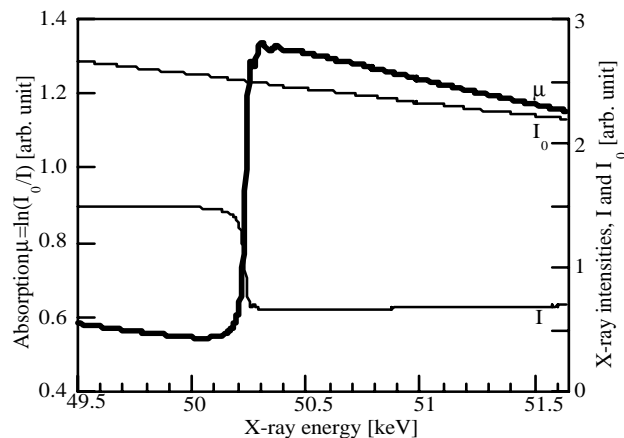


Figure 4
Raw Gd K -edge XAFS spectrum of $\text{Ce}_x\text{Gd}_{1-x}\text{O}_{(3+x)/2}$ ($x = 0.05$), incident and transmitted x-ray intensities, I_0 and I .

several hundreds eV limited by the subsequent L_{II} -edge. Monitored I_0 and I vs. E curves had no discontinuity as shown in this figure. This fact indicates that the present measurement system has been well tuned and worked for providing reliable x-ray spectra of Gd K -edge in all the specimens prepared in this work. We have obtained data of same quality also in Ce K -edge measurements on the specimens at $x > 0.2$. In Fig. 5, k^3 -weighted EXAFS function above the Gd K -edge of $\text{Ce}_x\text{Gd}_{1-x}\text{O}_{(3+x)/2}$ ($x = 0.05$) is shown, which demonstrates that the present measurements have provided EXAFS oscillation with good S/N ratios even in a wide k region, from 3.0 to 16.0. Figure 6 shows the radial distribution function (RDF) obtained by Fourier transform of the EXAFS function in Fig. 5, in which the phase shifts have not been considered. In this RDF corresponding to C-type crystal structure, the peak at 1.8 Å should be due to the interatomic distance of Gd-O (first shell).

The interatomic distances of Gd-O and Ce-O were obtained by least-square fitting with fixed coordination numbers of oxygen atoms ($\text{CN} = 2(3+x)$) using theoretical data including information of phase shifts calculated from FEFF (7.02) code (Zabinsky, 1995). In fitting process, we assumed that oxygen atoms surrounding a metal atom constitute a shell though the positions

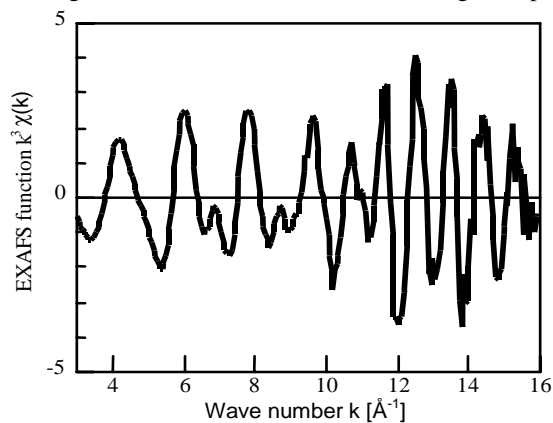


Figure 5
 k^3 weighted EXAFS function obtained from the data shown in Fig. 4.

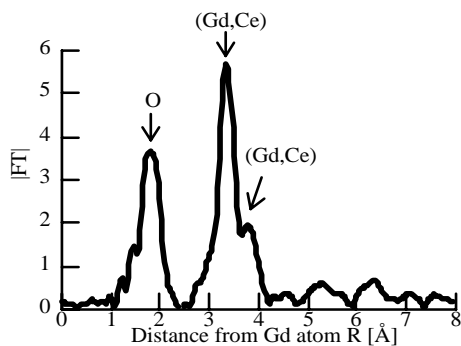


Figure 6
Fourier transform of the EXAFS function shown in Fig. 5.

of 6 oxygen atoms located around a metal in C-type oxide are classified 4 sites with slightly different metal-oxygen interatomic distances. R factors in all fitting processes were found to be less than 1.4%. Thus evaluated interatomic distances, $R_{\text{Gd-O}}$ and $R_{\text{Ce-O}}$, are plotted against x in Fig. 7, which indicates that $R_{\text{Gd-O}}$ and $R_{\text{Ce-O}}$ increase with cerium contents and $R_{\text{Gd-O}}$ are always larger than $R_{\text{Ce-O}}$ by about 0.1 Å. When the lattice parameter of C-type oxide is just twice as long as that of fluorite oxide, interatomic distance between metal and oxygen atom is shorter in C-type than in fluorite due to oxygen vacancies. The crystal structures of the binary oxides become close to fluorite type as x increases because of increase in oxygen contents by doping Ce. Therefore, Ce atoms introduced into C-type lattice would have lengthen both the interatomic distances. Average metal-oxygen interatomic distances calculated from linear combination of $R_{\text{Gd-O}}$ and $R_{\text{Ce-O}}$, $xR_{\text{Ce-O}} + (1-x)R_{\text{Gd-O}}$ are as well plotted and compared with those calculated from the lattice parameters determined with XRD. These two types of average interatomic distances well agree with each other. This agreement would support the idea that interatomic distances calculated the lattice parameters obtained by XRD correspond to the average values of the interatomic distances between respective metals and the nearest light elements even in solid solutions with a complex crystal structure

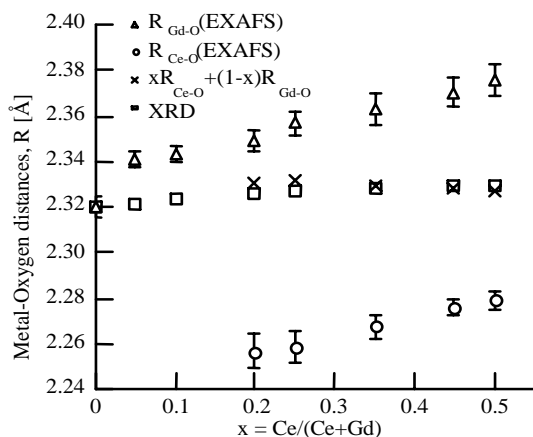


Figure 7
Ce-O and Gd-O interatomic distances, $R_{\text{Ce-O}}$ and $R_{\text{Gd-O}}$, determined with EXAFS analyses.
The linear combination values of $R_{\text{Ce-O}}$ and $R_{\text{Gd-O}}$ well agree with the average metal-oxygen distanced determined by XRD analyses.

like C-type. Details are in under consideration in terms of cluster models.

Summary of the present work is given as follows. X-ray absorption spectra near Ce and Gd K -edges in wide energy range (1.5 keV above K -edge energies) of binary oxide of $\text{Ce}_x\text{Gd}_{1-x}\text{O}_{(3+x)/2}$ ($0 \leq x \leq 0.5$) with C-type structure were measured. The interatomic distances of Gd-O and Ce-O, $R_{\text{Gd-O}}$ and $R_{\text{Ce-O}}$, increased with cerium contents and $R_{\text{Gd-O}}$ were larger than $R_{\text{Ce-O}}$. The linear combination values, $xR_{\text{Ce-O}} + (1-x)R_{\text{Gd-O}}$, well agreed with the average metal-oxygen interatomic distances obtained by XRD.

Acknowledgments

We thank the staff at SPring-8 for providing beam time and Dr. T. Uruga and Dr. H. Tanida for their help in the measurements at beamline BL01B1 at SPring-8. The present work was supported by the Research Foundation For Materials Science and Japan Society for the Promotion of Science under grant number 11780374.

References

- Inaba, H. & Tagawa, H. (1996). *Solid State Ion.* **83**, 1-16.
- Inaba, H., Sagawa, R., Hayashi, H. & Kawamura, K. (1999). *Solid State Ion.* **122**, 95-103.
- Kudo, T. & Obayashi, H. (1975). *J. Electrochem. Soc.* **122**(1), 142-147.
- Nakagawa, T., Yamamoto, T.A., Kitauji, Y., Kobayashi, Y., Katsura, M. & Emura, S. (1999). *Tech. Rep. of the Osaka Univ.* **49**, 209-215
- Ohashi, T., Yamazaki, S., Tokunaga, T., Arita, Y., Matsui, T., Harami, T. & Kobayashi, K. (1998). *Solid State Ion.* **113-115**, 559-564
- Uruga, T., Tanida, H., Yoneda, Y., Takeshita, K., Emura, S., Takahashi, M., Harada, M., Nishihata, Y., Kubozono, Y., Tanaka, T., Yamamoto, T., Maeda, H., Kamishima, O., Takabayashi, Y., Nakata, Y., Kimura, H., Goto, S. & Ishikawa, T. (1999). *J. Synchrotron Rad.* **6**, 143-145.
- Zabinsky, S.I., Rehr, J.J., Ankudinov, A., Albers, R.C. & Eller, M.J. (1995). *Phys. Rev. B.* **52**, 2995.